Organic Electronics 13 (2012) 2502–2507

Contents lists available at SciVerse ScienceDirect

Organic Electronics

journal homepage: www.elsevier.com/locate/orgel

Organic field-effect transistors as a test-bed for molecular electronics: A combined study with large-area molecular junctions

Kamal Asadi [a,*], Ilias Katsouras [b], Jan Harkema [b], Fatemeh Gholamrezaie [a,b], Edsger C.P. Smits [c], Fabio Biscarini [d], Paul W.M. Blom [b,c], Dago M. de Leeuw [a,b]

[a] Philips Research Laboratories, High Tech Campus 4, NL-5656 AE Eindhoven, The Netherlands
[b] Zernike Institute for Advanced Materials, University of Groningen, Nijenborgh 4, NL-9747 AG Groningen, The Netherlands
[c] Holst Centre, High Tech Campus 31, NL-5605 KN Eindhoven, The Netherlands
[d] CNR-Institute of Nanostructured Materials (ISMN), Via Gobetti 101, I-40129 Bologna, Italy

ARTICLE INFO

Article history:
Received 12 March 2012
Received in revised form 6 July 2012
Accepted 7 July 2012
Available online 2 August 2012

Keywords:
Charge injection
Self-assembled monolayer
Organic field-effect transistor
Molecular junction
Contact resistance
Tunneling

ABSTRACT

The contact resistance of a transistor using self-assembled monolayer (SAM)-modified source and drain electrodes depends on the SAM tunnel resistance, the height of the injection barrier and the morphology at the contact. To disentangle the different contributions, we have combined here the transmission line measurements in transistors with transport measurements of SAMs in large-area molecular junctions. The tunnel resistance of the SAM has been independently extracted in two-terminal large-area molecular junctions. We show that the tunneling resistance of the SAM can be added linearly to the contact resistance of the transistor with bare Au electrodes, to account for the increased contact resistance in the SAM-modified transistor. The observed agreement is discussed. The manifestation of the SAM in the contact resistance shows that transistors can potentially be used as an experimental test-bed for molecular electronics.

1. Introduction

The building block of organic electronic integrated circuits is the field-effect transistor (FET). Applications are envisaged in smart labels and active matrix displays [1]. The performance of the transistor depends on both charge injection and the transport of injected charges through the organic semiconductor [2]. The charge transport in organic semiconductors is theoretically well understood [3]. Experimentally, charge carrier mobilities close to unity ($cm^2/V\,s$) have been reported both for holes and electrons [4]. A remaining challenge is understanding of the charge injection mechanism.

To inject charge carriers the Fermi level of the metal electrode has to be aligned with either the lowest unoccupied molecular orbital (LUMO) or the highest occupied molecular orbital (HOMO) of the organic semiconductor [5]. An offset between these levels yields an injection barrier, the presence of which deteriorates charge injection [6–8]. To reduce the injection barrier the work function of the electrodes has been modified by using polar self-assembled monolayers [9]. This dipole layer can be described as two parallel sheets of charge separated by the length of the molecule. The change in workfunction of the modified electrode follows from classical electrostatics [10]. By adapting the dipole moment of the molecule the workfunction can be tuned in a range of about 2 eV.

Although control of charge injection with SAMs in FETs has led to improved performance, enhancement of the extracted field-effect mobility and reduction of the contact resistance [8,11], the role of SAMs on the FETs' performance is still elusive. In a thorough study, Stoliar et al. have investigated pentacene FETs with Au electrodes functionalized with alkanethiols. The extracted mobility increased with chain length up to $n = 8$ (n being the number of methylene units), and decreased exponentially for n larger than 8 [12]. This non-monotonic behavior,

* Corresponding author.
E-mail address: kamal.asadi@philips.com (K. Asadi).

1566-1199/$ - see front matter © 2012 Elsevier B.V. All rights reserved.
http://dx.doi.org/10.1016/j.orgel.2012.07.012

together with a clear odd–even fluctuation in the extracted mobility, has been explained as the result of the interplay between a decreased hole injection barrier due to the dipole moment of the SAM, the tunneling assisted by the SAM and by an improved morphology of the pentacene at the interface with the SAM.

Firstly, we note that the mobility extracted from transistors is rather tolerant for injection barriers. Pentacene has been investigated using transistors with source and drain electrodes with widely different work functions: Au, Cu, Ni. The saturated output currents differed by less than an order of magnitude. Experimentally, injection barriers as high as 1 eV can be surmounted [13,14].

Moreover, deposition of organic materials that tend to form crystalline domains is particularly sensitive to the surface energy of the substrate. Application of a SAM alters the surface energy and can therefore change the morphology of the deposited semiconductor [15]. Changes in device mobility upon application of a SAM are therefore not necessarily due to a change in injection barrier but can be due to a different morphology [16].

Finally, insertion of a SAM on the electrodes introduces an additional resistance. The extra resistance depends on the molecular structure of the SAM, conjugated or non-conjugated, and its molecular length [17,18]. The resistance increases with the molecular length, L, of the molecule as $R \propto \exp(\beta L)$, where the tunneling decay coefficient β depends on the energy gap between the HOMO and the LUMO [19,20]. Although the charge transport through single molecules has typically been investigated in break junctions, in scanning probe geometries and in large-area molecular junctions, Stoliar et al. extracted the decay coefficient β from transistor measurements [12]. However, how the SAM's resistance manifests in the overall resistance of the transistor remains unclear. It can be a simple series resistance or it can be a multiplication factor for the contact resistance.

Here, we combine electrical measurements in large-area molecular junctions and FETs to disentangle the different contributions of a SAM-modified electrode in the extracted mobility of a transistor. We used aliphatic SAMs because they are the benchmark for self-assembly. Aromatic SAMs can be applied to modify work-function and improve device performance. Therefore we speculate that the mechanism described for aliphatic SAMs would be same for aromatic SAMs. In order to eliminate the morphological complications, we used an amorphous semiconducting polymer. The electrode work function was tuned in opposite directions using SAMs with opposite dipole moments. We substantiate the effect of the SAM on the source drain electrodes in detail by investigation of the contact resistance of the FET using the transmission line method (TLM). We further corroborate on the role of the resistance of the SAM in a FET, by utilizing two-terminal large-area molecular junctions to independently extract the tunneling resistance of the used SAMs. We demonstrate that in a first order approximation the tunneling resistance of the SAM can be added linearly to the contact resistance of bare Au FETs, to account for the increased contact resistance in SAM-modified FETs. We tentatively propose that this result supports the claim that a FET can be used as an experimental test-bed for molecular electronics [12,18].

2. Experimental

2.1. Materials

Hexadecanethiol (HDT) was purchased from Aldrich and was distilled prior to use. Perfluorinated decanethiol (PFDT) was synthesized according to literature procedures [21]. Poly(2-methoxy-5-(2′-ethylhexyloxy)-1,4-phenylene vinylene) (MEH-PPV), an amorphous semiconducting polymer, was synthesized in our laboratory via the Gilch method [22]. Poly(3,4-ethylenedioxythiophene): poly(4-styrenesulphonic acid) (PEDOT:PSS) was purchased from AGFA. Chemical structures of all the compounds are given in Fig. 1c.

2.2. Device fabrication

FET test substrates (Fig. 1a) were fabricated on 150-mm highly p-type doped Si wafers with 250 nm thermally grown silicon oxide. Using conventional lithography, Au source and drain contacts (150 nm) were patterned with finger geometry with 5 nm of Ti as an adhesion layer. The channel length varied from 5 μm to 40 μm while the channel width was kept constant at 10,000 μm. Prior to use, the FET test substrates were treated with the primer hexamethyldisilazene (HMDS). HDT and PFDT were dissolved in ethanol with a concentration of 1 mM. The FET substrates were then immersed into the solution for 36 h. After the self-assembly process, the substrates were thoroughly rinsed with ethanol, toluene, and 2-propanol, respectively and then spin dried. MEH-PPV solution (dry toluene, 5 mg/ml) was then spin coated onto the FET substrates. The film thickness was kept at 100 nm. All spin coating and evaporation processes were performed in a nitrogen-filled glove box.

Large-area molecular junctions (Fig. 1b) were manufactured on 100-mm Si wafers with a 500 nm thermally grown oxide treated with HMDS. Au bottom electrodes of 60 nm (rms roughness was ~0.7 nm over an area of 0.25 μm^2) were thermally evaporated through a shadow mask with 1 nm of Cr as an adhesion layer. Vertical interconnects, ranging from 5 μm to 100 μm in diameter, were defined in a 570 nm layer of negative photoresist, ma-N1410 (micro resist technology GmbH) using conventional UV-lithography. SAM formation was identical to that of the FETs. After self-assembly, a 90 nm interlayer of PEDOT:PSS was spin coated onto the substrate and dried in dynamic vacuum. PEDOT:PSS acts as a highly conductive buffer layer that protects the SAM during evaporation of the 100 nm thick top Au contact. The top Au layer ensures better contact with the measurement probes and serves as a self-aligned mask for the removal of redundant PEDOT:PSS by reactive ion etching (O_2 plasma). This step eliminates any parasitic currents from the top to the bottom electrode.

For workfunction measurements, Au substrates were prepared by thermal evaporation of 150 nm of Au on ther-

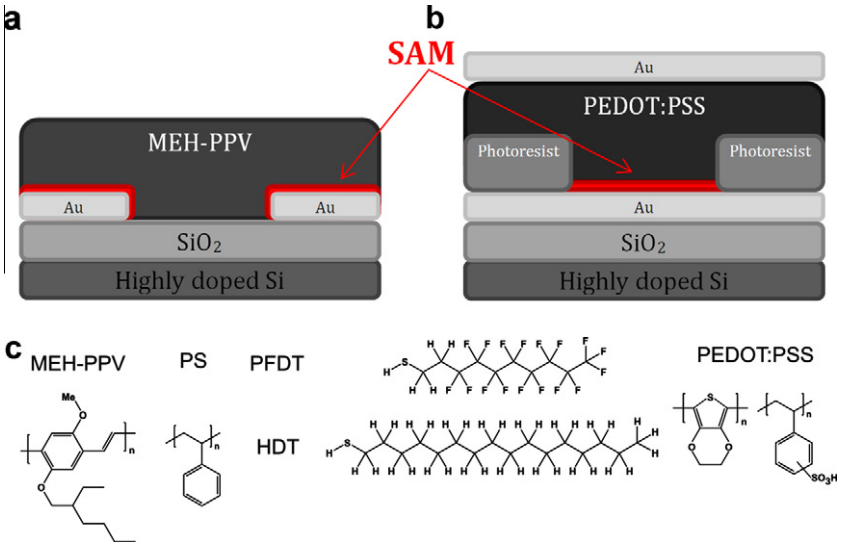

Fig. 1. Schematic of (a) a field-effect transistor and (b) a large-area molecular junction. The self-assembled monolayer (SAM) is indicated in red. (c) Chemical structure of the materials used.

mally grown SiO_2 substrate with 1 nm of Cr as an adhesion layer. After the self-assembly process the work function of bare and SAM-modified metals were measured using a Kelvin probe in a nitrogen-filled glove box.

2.3. Device characterization

Electrical measurements on FETs were all carried out in a probe station under high vacuum (10^{-6} mbar) with a Keithley 4200-SCS Semiconductor Characterization System. In the case of large-area molecular junctions, the probe station was pressurized at 10^{-6}–10^{-7} mbar for at least 6 h before the measurements to remove any residual water absorbed in the PEDOT:PSS layer [23]. The recorded current densities were averaged for approximately 40 devices with different diameters.

3. Results and discussion

We measured large-area molecular junctions with self-assembled monolayers of both PFDT and HDT, processed in identical conditions. In large-area molecular junctions the tunneling resistance can be evaluated by measuring the tunneling current [17]. Fig. 2 shows the tunneling current density versus applied voltage for PFDT and HDT junctions. The values are averaged over more than 40 devices. We calculated the normalized resistance in the Ohmic regime (RS, resistance × area, $\Omega\,\mu m^2$) at 0.1 V bias, corresponding to an electric field of 70 MV/m. The resistance scales linearly with device area for junctions of 5–100 μm in diameter, resulting in identical RS values. For HDT and PFDT SAMs the corresponding tunnel resistances were determined as $2.7 \times 10^6\ \Omega\,\mu m^2$ and $9.7 \times 10^5\ \Omega\,\mu m^2$, respectively.

We used bottom contact/bottom gate (BC/BG) transistors to extract the contact resistance in the FETs as a function of gate bias. In the coplanar BC/BG structure, charges

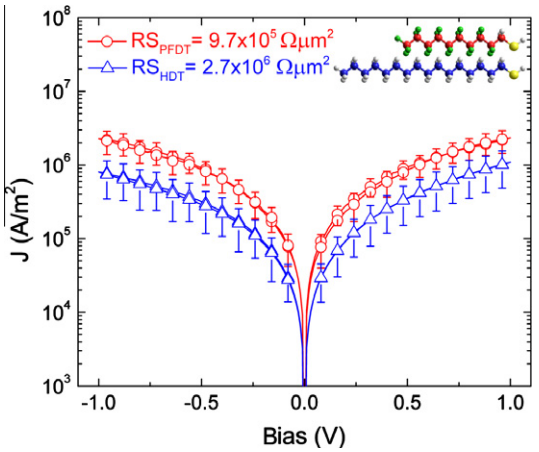

Fig. 2. Current density versus voltage as measured in large-area molecular junctions for PFDT and HDT. The values are averaged over more than 40 devices. The normalized resistance values (RS) and the corresponding structures of the molecules are indicated.

are directly injected into the accumulation layer at the semiconductor/dielectric interface, whereas in the staggered bottom contact/top gate (BC/TG) configuration, the source and drain electrodes are separated from the channel by the semiconducting layer, which yields a series resistance. Direct evaluation of SAM's tunnel resistance in BC/TG is then hampered by the presence of the additional resistance. Moreover, the current crowding effect in BC/TG impedes a good estimation of the effective contact area [24].

To unambiguously rule out the influence of an injection barrier we first focus on PFDT treated Au electrodes. The workfunction of bare Au was measured as 4.7–4.8 eV and that of the PFDT-treated Au electrode as 5.5 eV. The HOMO energy of MEH-PPV is approximately 5.1 eV. Therefore

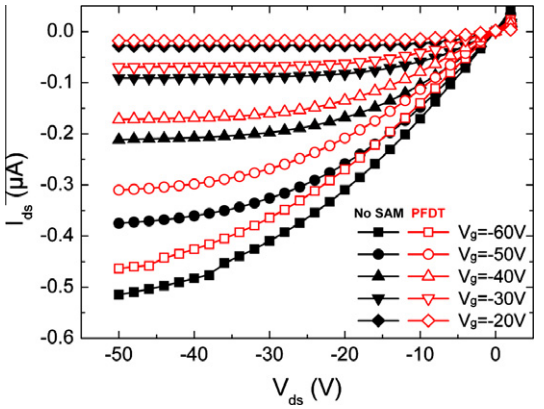

Fig. 3. Output characteristics of field-effect transistors with bare Au and PFDT-modified Au source drain electrodes in a bottom contact, bottom gate (BC/BG) configuration.

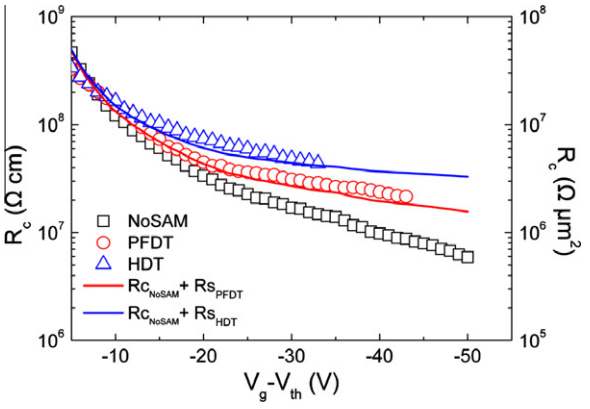

Fig. 4. Contact resistance of BC/BG transistors with bare Au and Au/PFDT treated electrodes as a function of gate bias. The contact resistances were derived from transmission line measurements using various channel lengths after correction for threshold voltage shifts. The channel width was kept constant at 10000 μm. The solid lines represent the summation of the tunnel resistance of corresponding SAM in molecular junctions with the contact resistance of the transistor with bare Au electrodes.

both bare Au and Au/PFDT electrodes form an Ohmic contact with MEH-PPV for hole injection.

The output characteristics are presented in Fig. 3. There is no hysteresis. The mobility determined for both transistors in the linear regime at small source drain bias is comparable and amounts to 3×10^{-4} cm^2/V s, in good agreement with reported mobility values. A similar value for the saturated mobility was determined from the transfer characteristics (not shown), which shows that that the channel resistance of the transistors with bare Au and Au/PFDT electrodes is the same.

Fig. 3 shows that the output current using Au/PFDT electrodes for all gate voltages is smaller than that using bare Au electrodes. The total device resistance is comprised of the channel resistance plus the contact resistances. To verify that the lower output current for Au/PFDT originates from an increased contact resistance, we derived the contact resistance using the TLM method by using transistors with various channel lengths [25]. The contact resistances derived from the TLM scaling analysis are presented in Fig. 4 as a function of gate bias. The contact resistance decreases with increasing negative gate bias as commonly observed [14,26,27]. At low bias the charges are injected into an undoped semiconductor yielding a high contact resistance. With increasing gate bias the semiconductor gets electrostatically doped, and the contact resistance decreases. The contact resistance has been presented as a function of mobility [26]. The determined value of the contact resistance in accumulation of about 10^8 Ω cm is lower than expected for a transistor with a mobility of 3×10^{-4} cm^2/V s, confirming the absence of any injection barrier.

Fig. 4 shows that the contact resistance increases when the Au source/drain electrodes are modified with a PFDT SAM. In order to relate the calculated contact resistance with the measured resistance of the PFDT SAM in molecular junctions, we renormalized the contact resistance to the injection area in transistors. The renormalized contact resistance (presented in Fig. 4 right axis) is taken as the contact resistance times the thickness of the accumulation layer which is typically estimated as about 2 nm [28].

In a simple approximation, we can reconstruct the contact resistance of the PFDT modified transistors by simply adding the tunnel resistance of the PFDT SAM as measured in large-area molecular junctions, to the renormalized contact resistance as determined in transistors using bare Au electrodes. The calculated curve is presented in Fig. 4 by the red line.[1] A good agreement with the extracted contact resistance of the PFDT modified transistor is obtained. At low gate bias, the contact resistance is dominated by charge injection into the undoped semiconductor. At higher gate bias, in accumulation, the contact resistance is dominated by the series resistance of the SAM.

To substantiate the analysis above, we varied the chemical nature of the SAM. We investigated transistors with HDT modified Au electrodes. The workfunction amounted to 4.1 eV yielding an injection barrier with MEH-PPV of approximately 1 eV. The contact resistance as a function of gate bias was obtained from TLM analysis and presented in Fig. 4. Despite the barrier of about 1 eV, the values are comparable to those of bare Au and PFDT treated electrodes. Transistors are tolerant for injection barriers due to the image-force lowering of the barrier caused by the high electric field at the source contact [29]. We added the measured tunnel resistance of HDT molecular junctions to that of renormalized contact resistance using bare Au electrodes. The blue line in Fig. 4 shows that a good agreement is obtained with the extracted contact resistance of transistors using HDT-modified electrodes. We note that, the agreement is surprising because resistance and Ohm's law are based on scattering and diffusive transport rather than tunneling. A tentative explanation is given below.

The absolute value of the resistance in a molecular junction depends on the nature of the electrical contacts to the molecule [30]. Strongly-coupled chemisorbed contacts

[1] For interpretation of color in Figs. 1 and 4, the reader is referred to the web version of this article.

yield lower resistances than weakly-coupled physisorbed contacts [31,32]. Furthermore, the metal work function and the composition of the chemical anchoring group can change the resistance [32,33]. Here we have determined the SAM resistance from molecular junctions that consist of a chemisorbed Au–S bottom contact, an alkane backbone and a physisorbed SAM/PEDOT:PSS top contact. The junction thickness is smaller than the electron coherence length and, therefore, Ohm's law is not obeyed. The electrical transport is by non-resonant tunneling. The resistance of a single molecule follows from e.g. multi barrier models yielding a resistance that is factorized with the contacts.

The total resistance of the transistor is the sum of the channel resistance and the contact resistance. At low bias the resistance is dominated by the channel resistance of the semiconductor. At high gate bias however the contact resistance dominates. In accumulation the semiconductor channel is electrostatically 'doped' by the gate voltage. Therefore, at sufficiently high gate voltage there are so many charge carriers in the channel that the semiconductors becomes degenerate and that it starts to act like an electrode at the SAM modified contact. The contact at low gate bias can be treated as a metal–insulator–semiconductor (MIS) tunnel junction. At high gate bias however the contact behaves as a MIM tunnel junction, similar as in the large-area molecular junctions [34]. Here we add the absolute value of the SAM resistance as a series resistance to the total resistance of the transistor without SAM. The resistance of the molecular junction is factorized with the PEDOT:PSS resistance [35]. However, when using highly conductive PEDOT:PSS and optimized processing the absolute resistance derived agrees with that of break junction and C-AFM measurements [36]. The agreement obtained here might be due to the fact that the junction consists of metal/SAM/doped semiconductor. Therefore, the SAM resistance is clearly manifested in the contact resistance of the transistors. Hence a SAM-modified transistor can be used as an experimental test-bed for molecular electronics as first proposed by Stoliar et al. [12].

4. Conclusion

The contact resistance of a transistor using SAM-modified source and drain electrodes depends on the SAM tunnel resistance, the height of the injection barrier and the morphology at the contact. To disentangle the different contributions, we have combined transmission line measurements in transistors with transport measurements of SAMs in large-area molecular junctions. In order to eliminate the morphological complications, we have used in the transistor an amorphous semiconducting polymer, MEH-PPV. To unambiguously rule out the influence of an injection barrier we have focused on PFDT-treated Au electrodes. Both bare Au and Au/PFDT electrodes form an Ohmic contact with MEH-PPV for hole injection. However, the output current using Au/PFDT electrodes is slightly lower than that using bare Au electrodes due to higher contact resistance. The absolute value of the contact resistance in combination with the extracted device mobility confirms the absence of any injection barrier.

The tunnel resistance of the PFDT SAM has been independently extracted in two-terminal large-area molecular junctions. We show that in first order approximation the tunneling resistance of the SAM can be added linearly to the contact resistance of the bare Au transistor, to account for the increased contact resistance in the PFDT-modified transistor. The analysis has been verified by using different SAMs.

The SAM modified contact at low gate bias can be treated as a metal–insulator–semiconductor (MIS) tunnel junction. At high gate bias however the contact behaves as a MIM tunnel junction, similar as in the large-area molecular junctions.

The agreement obtained here shows that the SAM resistance is clearly manifested in the contact resistance of the transistors. Hence SAM-modified transistors can potentially be used as a gauge to measure electrical transport through single molecules.

Acknowledgments

The authors wish to thank both Zernike Institute for Advanced Materials and the EU project ONE-P, No. 212311 for financial support.

References

[1] (a) E. Cantatore, T.C.T. Geuns, G.H. Gelinck, E. van Veenendal, A.F.A. Gruijthuijsen, L. Schrijnemakers, S. Drews, D.M. de Leeuw, J. Solid-State Circuits 42 (2007) 84;
(b) D.M. de Leeuw, E. Cantatore, Mater. Sci. Semicon. Proc. 11 (2008) 199.
[2] B. Crone, A. Dodabalapur, Y.-Y. Lin, R.W. Filas, Z. Bao, A. LaDuca, R. Sarpeshkar, H.E. Katz, W. Li, Nature 403 (2000) 521.
[3] (a) C. Tanase, E.J. Meijer, P.W.M. Blom, D.M. de Leeuw, Phys. Rev. Lett. 91 (2003) 216601;
(b) M.C.J.M. Vissenberg, M. Matters, Phys. Rev. B 57 (1998) 12964;
(c) H. Bässler, Phys. Stat. Sol. B 175 (1993) 15;
(d) W.F. Pasveer, J. Cottaar, C. Tanase, R. Coehoorn, P.A. Bobbert, P.W.M. Blom, D.M. de Leeuw, M.A.J. Michels, Phys. Rev. Lett. 94 (2005) 206601;
(e) H. Sirringhaus, Adv. Mater. 17 (2005) 2411.
[4] (a) H. Yan, Z. Chen, Y. Zheng, C. Newman, J.R. Quinn, F. Dotz, M. Kastler, A. Facchetti, Nature 457 (2009) 679;
(b) Z. Chen, M.J. Lee, R. Shahid Ashraf, Y. Gu, S. Albert-Seifried, M. Meedom Nielsen, B. Schroeder, T.D. Anthopoulos, M. Heeney, I. McCulloch, H. Sirringhaus, Adv. Mater. 24 (2012) 647.
[5] (a) G. Horowitz, P. Lang, M. Mottaghi, H. Aubin, Adv. Funct. Mater. 14 (2004) 1069;
(b) N. Koch, Chem. Phys. Chem. 8 (2007) 1438.
[6] K. Asadi, F. Gholamrezaie, E.C.P. Smits, P.W.M. Blom, B. de Boer, J. Mater. Chem. 17 (2007) 1947.
[7] (a) I.H. Campbell, J.D. Kress, R.L. Martin, D.L. Smith, N.N. Barashkov, J.P. Ferraris, Appl. Phys. Lett. 71 (1997) 3528;
(b) S. Khodabakhsh, D. Poplavskyy, S.Heutz.J. Nelson, D.D.C. Bradley, H. Murata, T.S. Jones, Adv. Funct. Mater. 14 (2004) 1205.
[8] B.H. Hamadani, D.A. Corley, J.W. Ciszek, J.M. Tour, D. Natelson, Nano Lett. 6 (2006) 1303.
[9] B. de Boer, A. Hadipour, M.M. Mandoc, T. Van Woudenbergh, P.W.M. Blom, Adv. Mater. 17 (2005) 621.
[10] J.C. Love, L.A. Estroff, J.K. Kriebel, R.G. Nuzzo, G.M. Whitesides, Chem. Rev. 105 (2005) 1103.
[11] H. Ma, H.L. Yip, F. Huang, A.K.Y. Jen, Adv. Funct. Mater. 20 (2010) 1371.
[12] P. Stoliar, R. Kshirsagar, M. Massi, P. Annibale, C. Albonetti, D.M. de Leeuw, F. Biscarini, J. Am. Chem. Soc. 129 (2007) 6477.
[13] (a) D.J. Gundlach, L. Zhou, J.A. Nichols, T.N. Jackson, P.V. Necliudov, M.S. Shur, J. Appl. Phys. 100 (2006) 024509;
(b) E.C.P. Smits, T.D. Anthopoulos, S. Setayesh, E. van Veenendaal, R. Coehoorn, P.W.M. Blom, B. de Boer, D.M. de Leeuw, Phys. Rev. B 73 (2006) 205316;

(c) L. Bürgi, M. Turbiez, R. Pfeiffer, F. Bienewald, H.-J. Kirner, C. Winnewisser, Adv. Mater. 20 (2008) 2217.
[14] T.D. Anthopoulos, C. Tanase, S. Setayesh, E.J. Meijer, J.C. Hummelen, P.W.M. Blom, D.M. de Leeuw, Adv. Mater. 16 (2004) 2174.
[15] (a) M. Chiodi, L. Gavioli, M. Beccari, V. Di Castro, A. Cossaro, L. Floreano, A. Morgante, A. Kanjilal, Phys. Rev. B 77 (2008) 115321;
(b) Y. Ge, J.E. Whitten, J. Phys. Chem. C 112 (2008) 1174.
[16] (a) C. Bock, V. Pham, U. Kunze, D. Kafer, G. Witte, A. Terfort, Appl. Phys. Lett. 91 (2007) 052110;
(b) K. Asadi, Y. Wu, F. Gholamrezaie, P. Rudolf, P.W.M. Blom, Adv. Mater. 21 (2009) 4109;
(c) J. Gundlach, J.E. Royer, S.K. Park, S. Subramanian, O.D. Jurchescu, B.H. Hamadani, A.J. Moad, R.J. Kline, L.C. Teague, O. Kirillov, C.A. Richter, J.G. Kushmerick, L.J. Richter, S.R. Parkin, T.N. Jackson, J.E. Anthony, Nat. Mater. 7 (2008) 216;
(d) F. Gholamrezaie, K. Asadi, R.A.H.J. Kicken, B.M.W. Langeveld-Voss, D.M. de Leeuw, P.W.M. Blom, PWM, Synth. Metals 161 (2011) 2226.
[17] (a) H.B. Akkerman, P.W.M. Blom, D.M. de Leeuw, B. de Boer, Nature 441 (2006) 69;
(b) S.H. Choi, B. Kim, C.D. Frisbie, Science 320 (2008) 1482.
[18] S. Casalini, A. Shehu, S. Destri, W. Porzio, M.C. Pasini, F. Vignali, F. Borgatti, C. Albonetti, F. Leonardi, F. Biscarini, Org. Electron. 13 (2012) 789.
[19] A. Salomon, D. Cahen, S. Lindsay, J. Tomfohr, V.B. Engelkes, C.D. Frisbie, Adv. Mater. 15 (2003) 1881.
[20] H.B. Akkerman, B. de Boer, J. Phys.: Condens. Matter 20 (2008) 013001.
[21] C. Naud, P. Calas, H. Blancou, A. Commeyras, J. Fluorine Chem. 104 (2000) 173.
[22] K. Asadi, J. Wildeman, P.W.M. Blom, D.M. de Leeuw, IEEE Trans. Electron. Dev. 57 (2010) 3466.
[23] I. Katsouras, A.J. Kronemeijer, E.C.P. Smits, P.A. van Hal, T.C.T. Geuns, P.W.M. Blom, D.M. de Leeuw, Appl. Phys. Lett. 99 (2011) 013303.
[24] T.J. Richards, H. Sirringhaus, J. Appl. Phys. 102 (2007) 094510.
[25] (a) D.J. Gundlach, L. Jia, T.N. Jackson, IEEE Electron. Dev. Lett. 22 (2001) 571;
(b) B.H. Hamadani, D.A. Corley, J.W. Ciszek, J.M. Tour, D. Natelson, Nano Lett. 6 (2006) 1303.
[26] E.J. Meijer, G.H. Gelinck, E. van Veenendaal, B.-H. Huisman, D.M. de Leeuw, T.M. Klapwijk, Appl. Phys. Lett. 82 (2003) 4576.
[27] F. Torricelli, J.R. Meijboom, E.C.P. Smits, A.K. Tripathi, M. Ferroni, S. Federici, G.H. Gelinck, L. Colalongo, Z.M. Kovács-Vajna, D.M. de Leeuw, E. Cantatore, IEEE Trans. Electron. Dev. 58 (2011) 2610.
[28] (a) G. Horowitz, M.E. Hajlaoui, R. Hajlaoui, J. Appl. Phys. 87 (2000) 4456;
(b) C. Tanase, E.J. Meijer, P.W.M. Blom, D.M. de Leeuw, Org. Electron. 4 (2003) 33.
[29] J.J. Brondijk, F. Torricelli, E.C.P. Smits, P.W.M. Blom, D.M. de Leeuw, Org. Electron. 13 (2012) 1526.
[30] (a) K.W. Hipps, Science 294 (2001) 536;
(b) J.G. Kusherick, Mater. Today 8 (7) (2005) 26;
(c) D. Vuillaume, S. Lenfant, Microelectron. Eng. 70 (2003) 539.
[31] X.D. Cui, A. Primak, X. Zarate, J. Tomfohr, O.F. Sankey, A.L. Moore, T.A. Moore, D.A. Gust, G. Harris, S.M. Lindsay, Science 294 (2001) 571.
[32] V.B. Engelkes, J.M. Beebe, C.D. Frisbie, J. Am. Chem. Soc. 126 (2004) 14287.
[33] (a) F. Chen, X. Li, J. Hihath, Z. Huang, N.J. Tao, J. Am. Chem. Soc. 128 (2006) 15874;
(b) J.M. Beebe, V.B. Engelkes, L.L. Miller, C.D. Frisbie, J. Am. Chem. Soc. 124 (2002) 11268;
(c) Y.S. Park, A.C. Whalley, M. Kamenetska, M.L. Steigerwald, M.S. Hybertsen, C. Nuckolls, L. Venkataraman, J. Am. Chem. Soc. 129 (2007) 15768.
[34] S.M. Sze, Physics of Semiconductor Devices, Wiley, New Jersey, 2007.
[35] A.J. Kronemeijer, I. Katsouras, E.H. Huisman, P.A. van Hal, T.C.T. Geuns, P.W.M. Blom, D.M. de Leeuw, Small 7 (2011) 1593.
[36] P.A. Van Hal, E.C.P. Smits, T.C.T. Geuns, H.B. Akkerman, B.C. De Brito, S. Perissinotto, G. Lanzani, A.J. Kronemeijer, V. Geskins, J. Cornil, P.W.M. Blom, B. de Boer, D.M. de Leeuw, Nat. Nanotechnol. 3 (2008) 749.